ACS Catalysis

Research Article

pubs.acs.org/acscatalysis

Reaction Behaviors and Kinetics during Induction Period of Methanol Conversion on HZSM-5 Zeolite

Liang Qi,[†,‡] Yingxu Wei,[†] Lei Xu,[*,†] and Zhongmin Liu[*,†]

[†]National Engineering Laboratory for Methanol to Olefins, Dalian National Laboratory for Clean Energy, iChEM (Collaborative Innovation Center of Chemistry for Energy Materials), Dalian Institute of Chemical Physics, Chinese Academy of Sciences, Dalian 116023, People's Republic of China

[‡]University of Chinese Academy of Sciences, Beijing 100049, People's Republic of China

Supporting Information

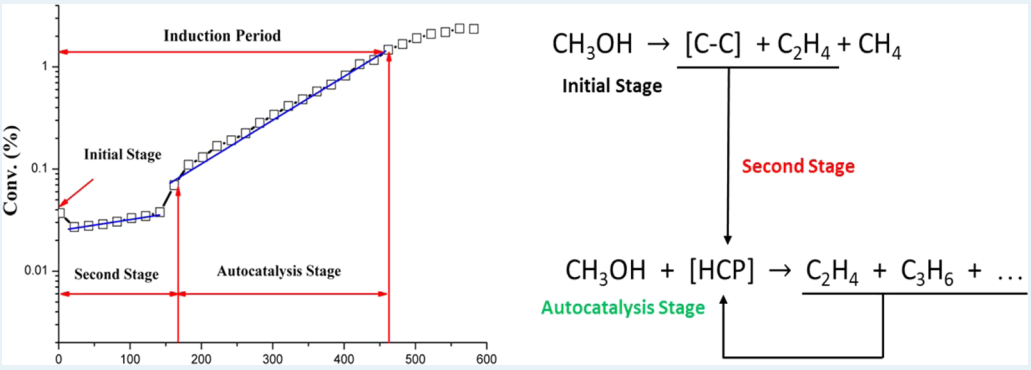

ABSTRACT: The reaction behavior in the induction period of the methanol to hydrocarbon (MTH) reaction over HZSM-5 (Si/Al = 19) zeolite has been investigated in a fixed-bed reactor. It is found that the induction period could be more than 2 h when the reaction was performed at a temperature of 255 °C and below. Meanwhile, three reaction stages can be clearly distinguished in the induction period: i.e., the initial C−C bond formation stage, the hydrocarbon pool (HCP) species formation stage, and the autocatalysis reaction stage. For each reaction stage, the kinetic parameters as well as the apparent activation energies have been evaluated. The HCP species formation stage is shown to be the rate-determining step. Addition of a ppm amount (molar) of benzene, toluene, or *p*-xylene to the methanol feed leads to a shortened induction period due to a lower energy barrier for both the HCP species formation and the autocatalysis reaction. A critical value of HCP species, $[HCP]_c$, that is required for starting the autocatalysis reaction (the third stage) has been proposed. This critical value was measured to be 1 toluene molecule per 276 unit cells for HZSM-5 zeolite when toluene is cofed with methanol.

KEYWORDS: *methanol, induction period, kinetics, activation energy, HZSM-5*

INTRODUCTION

The methanol to hydrocarbon (MTH) reaction has received considerable attention in recent years, as it can be developed into an industrial process that transforms methanol, which can be readily obtained from nonoil feedstock including coal and natural gas, to desired hydrocarbons such as olefins and aromatics. The methanol to olefins (MTO) reaction is one of the most important MTH processes and has been recently commercialized.[1]

The MTH reaction, involving first the formation of a C−C bond, carbon chain growth, alkylation and polycondensation of light olefins, and coke formation due to hydrogen transfer reactions, has been demonstrated to be quite complicated.[2,3] Previous studies have shown that three stages appear in the MTH reaction: i.e. the induction period, the steady-state reaction period, and the deactivation period.[1] However, detailed information on the MTH reaction is still absent due to rapid secondary reactions on one hand and lack of suitable techniques monitoring these rapid reactions on the other. Recent studies have verified that the hydrocarbon pool (HCP) mechanism is dominant in the steady-state period in the MTH reaction. This mechanism suggests that methanol molecules react with hydrocarbon species diffused into the catalyst, which initializes a sequence of steps leading to the formation of primary olefin products as well as the regeneration of the original HCP species in a catalytic cycle.[4−14] The HCP mechanism will not work until sufficient reaction centers that are necessary for starting the autocatalysis are formed. The stage before the HCP mechanism starts to work is the so-called induction period.[3] On the basis of the HCP mechanism, two reaction routes have been proposed to explain the MTH reaction pathway: namely, the side-chain methylation route and

Received: March 27, 2015
Revised: May 21, 2015
Published: May 22, 2015

DOI: 10.1021/acscatal.5b00654
ACS Catal. 2015, 5, 3973−3982

the paring route.[15,16] Specifically, the paring route involves the contraction of six-membered-ring cations and the expansion of five-membered-ring cations that split off alkenes.[17] In contrast, the side-chain methylation route proceeds via the methanol methylation on polymethylbenzenium cations and the subsequent elimination of side-chain groups to produce olefins. In both ways, carbenium ions are believed to be the important intermediates to produce olefins. Recently, investigations of the intermediates have made good progress.[18−23] In DNL-6, a newly synthesized SAPO-type molecular sieve with large cavities, heptamethylbenzenium cation (heptaMB$^+$) was directly observed for the first time during methanol conversion under real reaction conditions.[24] Meantime, heptaMB$^+$ and another very important carbenium ion involved in the MTH reaction, the pentamethylcyclopentyl cation (pentaMCP$^+$), were also found in the MTH reaction over CHA-type catalysts.[25] A study by Bjorgen et al. found that, in addition to polymethylbenzenes, olefins may also act as another kind of active HCP species in zeolites such as ZSM-5 with 3-D and 10-ring channels.[26,27] This led to the establishment of the "dual-cycle" mechanism: an aromatics-based cycle produces ethene and methylbenzenes, and an olefin-based methylation/cracking cycle produces C_3^+ olefins.[26,27]

Although both the HCP mechanism and the dual-cycle mechanism can explain the MTH reaction in the steady-state period, they do not involve the initial hydrocarbon formation: i.e., the formation of the first C−C bond and initial HCP species. In past few decades, more than 20 direct mechanisms (such as the oxonium ylide mechanism, carbene mechanism, carbocation mechanism, and methane−formaldehyde mechanism) for the first C−C bond generation in the MTH reaction have been proposed,[2,28,29] most of which, however, lack direct experimental evidence.[30,31] Some experimental[32−49] and theoretical works[28,29,50−60] suggest that the surface methoxy species act as a source of primary hydrocarbons during the induction period the of MTH reaction over acidic zeolite catalysts, in which the direct observations of the first C−C bond are still missing. In a very recent study Fan et al. found the formation of $CH_3OCH_2^+$ intermediate species in the initial stage and proposed that propene is the first alkene product which induced the HCP mechanism.[61] However, the direct trapping of 1,2-dimethoxyethane by GC-MS or other techniques requires further investigation.[61] In addition, detailed research on the formation of the first reaction center is also desired to clarify the initiation of the MTH reaction.

Direct observation of the induction period is difficult when methanol conversion is high, since the reaction can proceed rapidly once some cyclic species form or some coke deposits on the catalyst surface. Several groups have studied the MTH induction period.[62−66] A consecutive pulse reaction system was designed in our laboratory to directly observe the reaction behavior at the very beginning of methanol conversion. It was found that for short contact times methanol in the induction period was converted with a high methane yield. The contact time mainly influences the formation of primary organic compounds in the induction period.[62] Dai and coworkers recently observed several initial active species and found their relationships with other benzene-based carbenium ions in the induction period of the MTH reaction over SAPO-41 and SAPO-34 catalyst.[63,64] Langner et al. studied the effect of the prior introduction of olefin precursors on the subsequent methanol conversion and found that, at reaction temperatures below 300 °C, the MTH induction period could be shortened by adding a very small amount of olefin precursors, especially cyclohexanol.[65] Lee and coworkers demonstrated the effect of crystallite size on the MTH induction period over SAPO-34 catalyst. The large-crystal catalyst with smaller external surface area presents a longer induction period, which has been attributed to the smaller number of accessible channels near the external surface.[66] These studies certainly favor the understanding of initial HCP species formation during the methanol conversion reaction; however, the mechanism of the induction period in the MTH reaction is still unclear.

If the induction period in the MTH reaction is considered as a process during which the organic-free zeolite catalyst is transferred to a working catalyst, the methanol conversion at this stage would be quite low (close to 0). Under normal reaction conditions where the methanol conversion is high, the induction period could hardly be observed. It is also difficult to monitor the change in catalyst because of the current limitations of the instruments and analysis methods. In this research, we studied the MTH reaction at temperatures lower than 255 °C. It is found that the induction period of the MTH reaction over HZSM-5 catalyst could be largely extended by decreasing the reaction temperature, and the induction period could be as long as several hours when the temperature is lower than 255 °C. This enabled us to investigate the reaction process and kinetic behavior in the MTH induction period. Moreover, the effect of trace amounts of aromatic additives on the MTH induction period has also been studied.

EXPERIMENTAL SECTION

HZSM-5 (Si/Al = 19) was obtained from the Catalyst Plant of Nankai University (Tianjin, People's Republic of China). The zeolite sample was first pressed into tablets and then crushed and sieved into a fraction of 40−60 mesh. Methanol (>99.9%), benzene (>99.5%), toluene (>99.5%), and *p*-xylene were all purchased from commercial sources at the highest purity available. The reactions were performed in a fixed-bed stainless steel tubular reactor (9 mm i.d.) under atmospheric pressure. In all experiments, a catalyst sample of 1.0 g was loaded into the reactor. Quartz sand was added to the upper and lower parts of the reactor to get a plug flow of the mixed feed. Prior to the introduction of reactants, the catalyst was activated in situ at 550 °C under a flow of 20 mL min^{-1} of helium for 1 h before cooling to the desired reaction temperature. The reactants were pumped steadily into the reactor at a rate of 0.085 mL min^{-1}. The effluent was analyzed by an online gas chromatograph (Angilent GC7890A) equipped with an FID detector and a PoraPLOT Q-HT capillary column.

The conversion in this work refers to the percent of methanol converted into hydrocarbons, and dimethyl ether in the effluent is considered as a reactant.

RESULTS AND DISCUSSION

General Phenomenon of the Induction Period of MTH Reaction. Figure 1 shows the change in methanol conversion with time on stream (TOS) for different reaction temperatures (245−280 °C). The temperature affects the induction period significantly. At 280 °C, the methanol conversion at 2 min is negligibly low and then increases rapidly to ca. 37% at 22 min, which means an obvious induction period exists in the MTH reaction. At a lower temperature of 270 °C, the methanol conversion at 22 min is only 1% and then increases gradually to 26% at 62 min. This suggests that a lower reaction temperature

DOI: 10.1021/acscatal.5b00654
ACS Catal. 2015, 5, 3973−3982

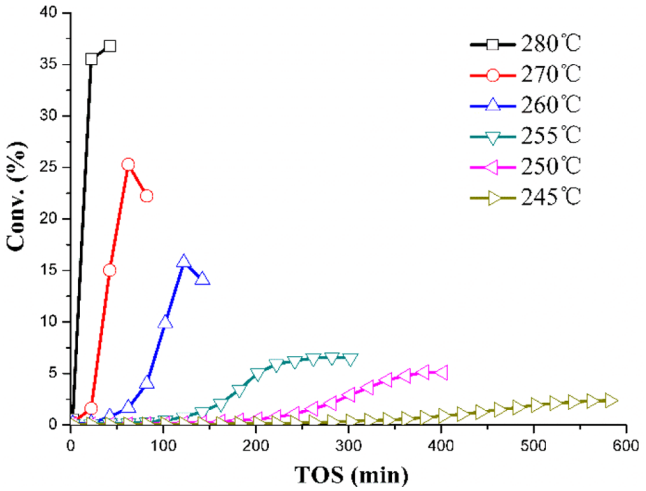

Figure 1. Conversion of methanol over HZSM-5 zeolite as a function of TOS for different reaction temperatures.

prolongs the induction period. The induction period could be as long as several hours when the temperature is lower than 255 °C. In case of 245 °C, apparent methanol conversion has not been found until 300 min.

The methanol conversion and product distribution at 245 °C are shown in Figure 2 as a function of TOS. It is interesting to note that, if the methanol conversion is plotted with a logarithmic scale, three different stages can be distinguished

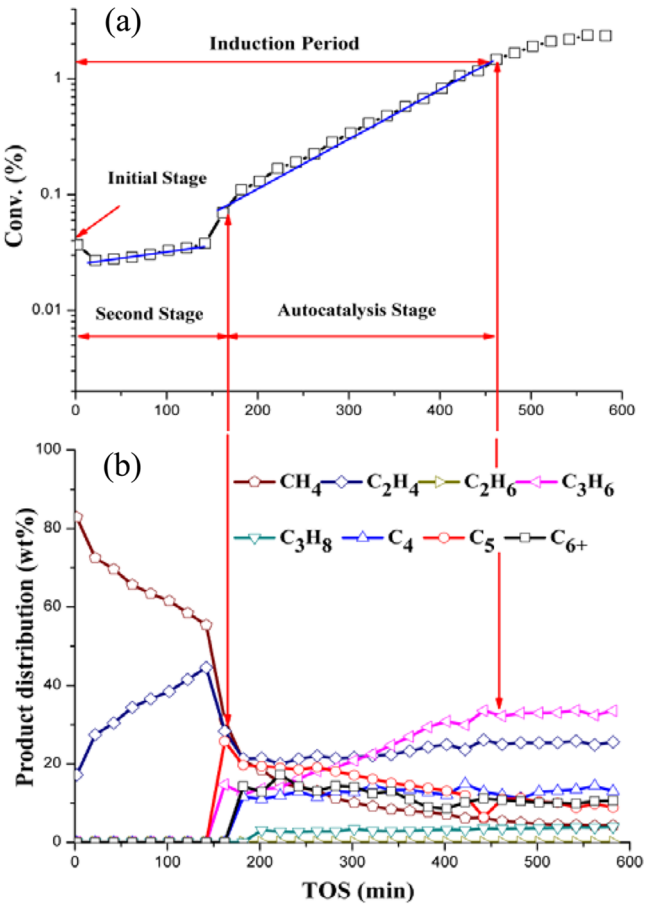

Figure 2. Conversion of methanol (a) and product distribution (b) over HZSM-5 zeolite at 245 °C as a function of TOS.

(Figure 2a). At the second and third stages the methanol conversion shows an exponential dependence (or linear dependence at a logarithmic scale) on TOS (Figure 2a). The second stage appears after a short reaction time and extends for a long time with a low level of methanol conversion (<0.03%). The third stage arises with a greater slope and shows the feature of autocatalysis. Correspondingly, as can be seen from Figure 2b, the initial hydrocarbon products at 2 min are mainly methane and its fraction in the products decreases in the last two stages. Considering the H/C ratio and atom balance, one can deduce that some hydrogen-poor substances formed on the catalyst because of the high fraction of methane in the products. C_2H_4 is obviously the first detectable olefin product, and C_3H_6 and C_5 are not measured until 162 min. The appearance and rapid increase of C_3H_6 and C_5 are at the beginning of the second stage. From Figure 2, it can be argued that the induction period involves three reaction stages. It is tentatively proposed that the first stage can be attributed to the first C−C bond formation, the second stage corresponds to the formation and accumulation of HCP species, and the third stage appears after sufficient HCP substances are formed, and the HCP species start to play an important role in the reaction; thus, the autocatalysis initiates.

It has been documented that, at very low methanol conversion (below 0.1%), the ratio of carbon selectivity of ethene to propene is close to 1.[67,68] In an early report, Haag et al. found that with ZSM-5 catalyst of SiO_2/Al_2O_3 = 35−70, the molar ratio of propene to ethane was 1 or greater when the conversion was about 0.05%.[69] In the present study, however, propene was not detected and ethene was the only gas product containing a C−C bond during the long induction period. However, at the first stage, ethene may not be the only species that contains a C−C bond. Some other species containing a C−C bond ([C−C]) may also exist on the surface of the catalyst, which cannot be detected with GC analysis. As a result, the formation of initial HCP species is considered very complicated, and it may include ethene methylation, ethene dimerization, an ethene reaction with [C−C], or a combination of these reactions. When the HCP species accumulate to a critical amount, the HCP mechanism will start to work. This leads to efficient olefin production and in turn speeds up the formation of HCP species and further accelerates methanol conversion in an autocatalysis way. Thereafter, the methanol conversion is further enhanced by the aromatics-based cycle where, however, the olefin methylation route cannot be excluded. Accordingly, we proposed the MTH induction reaction as a kinetic process, as shown in Scheme 1.

Although the induction period is long enough under the condition of low reaction temperature, monitoring the HCP species in the catalyst is still a hard task. This is due to the very low methanol conversion and HCP species concentration at the first and second stages. In principle, the formation of the first product containing a C−C bond and further reactions such as olefin methylation, olefin polymerization, hydrogen transformation, and aromatization can also happen. A close check with the time and methanol conversion for each reaction stage in the induction period indicates that the reaction rate is possibly controlled by the formation step of HCP species. However, there is possibly overlap between the first stage and the second stage, and thus the rate-determining step is hard to determine without kinetic information.

DOI: 10.1021/acscatal.5b00654
ACS Catal. 2015, 5, 3973−3982

Scheme 1. Three-Stage MTH Induction Reaction Mechanism

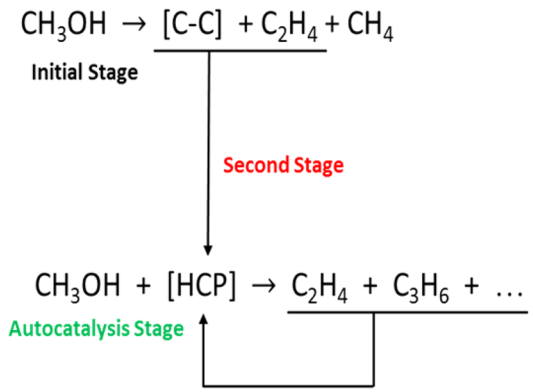

Kinetics in the Induction Period. *Kinetics and Activation Energy of the Initial Stage.* The rate expression for methanol conversion in the initial stage can be defined as

$$dx/dt = k_1(1 - x)^n \quad (1)$$

where x is the methanol conversion, t is the reaction time, k_1 is the rate constant, and n is the reaction order. At this initial stage, the methanol conversion is very low and is not dependent on the methanol concentration, which leads to a zero-order reaction: i.e., $n = 0$. The kinetic equation can be further simplified to be

$$dx = k_1\, dt \quad (2)$$

At the very beginning of the reaction when $t = 0$, the methanol conversion should be 0. After integration of the equation from $t = 0$ to t_i and corresponding methanol conversion $x = 0$ to x_i, the equation is

$$k_1 = \frac{x_i}{t_i} \quad (3)$$

By use of the methanol conversion at $t = 2$ min, the rate constant k_1 at different reaction temperatures could be calculated, as shown in Table1.

The Arrhenius plot of ln k_1 as a function of $1/T$ is shown in Figure 3, giving a perfect straight line. On the basis of the slope of the line, the activation energy for the first stage of the MTH induction period can be readily calculated. The calculated activation energy for the first stage is 153 kJ mol^{-1}, which is close to the theoretical predictions for first C−C bond formation in methanol conversion processes.[28,29,31]

Kinetics and Activation Energy of the Second Stage. For the second stage, methane is still the major product, implying the simultaneous generation of the initial HCP species. The hydrogen-rich methane formation is accompanied by the hydrogen-poor hydrocarbon residing on the catalyst. On the basis of the profile of methanol conversion and the product distribution with TOS, it can be deduced that a certain amount of HCP species is required to start the autocatalysis reaction. This will be further confirmed by our experimental results discussed in Effect on the Methanol Conversion, where it is found that the addition of a very small amount of aromatics could shorten the second reaction stage. During this stage, both the methanol conversion and the concentration of the HCP species are quite low, and the HCP formation reaction can also be considered as a zero-order reaction for methanol concentration. The rate expression for HCP species formation is

$$d[\mathrm{HCP}] = k_2^{\mathrm{i}}\, dt \quad (4)$$

where [HCP] is the content or concentration of HCP species in ZSM-5 zeolite and k_2^{i} is the intrinsic reaction rate constant for the formation of HCP species. As discussed above, the concentration of HCP species reaches a critical value, $[\mathrm{HCP}]_c$, after the time t_c. By integrating on both sides of eq 4, we can obtain

$$\int_0^{[\mathrm{HCP}]_c} d[\mathrm{HCP}] = k_2^{\mathrm{i}} \int_0^{t_c} dt \quad (5)$$

$$\frac{k_2^{\mathrm{i}}}{[\mathrm{HCP}]_c} = \frac{1}{t_c} \quad (6)$$

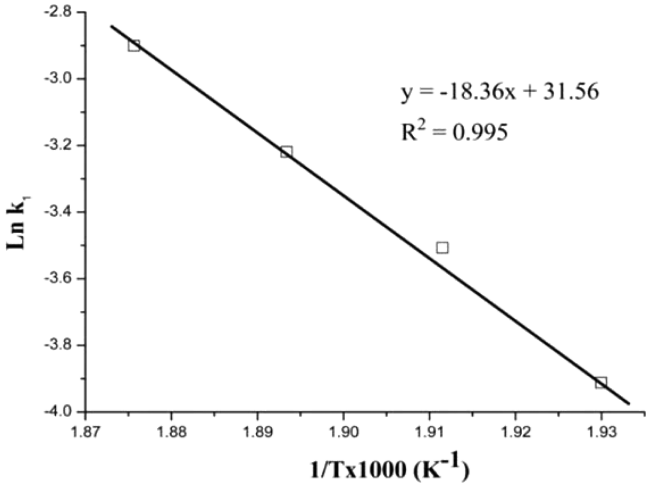

Figure 3. Arrhenius plot: rate constant for the first-stage reaction in the MTH induction period in the temperature range 245−260 °C.

Table 1. Kinetic Parameters of Three Stages

	temp (°C)				
reaction stage	245	250	255	260	E (kJ mol^{-1})
first stage					
k_1	0.0185	0.02795	0.03795	0.055	153
second stage					
t_c/min	162	82	42	22	301
k_2	0.006173	0.01219	0.02381	0.04545	
third stage					
k_3	0.010	0.015	0.028	0.043	234

DOI: 10.1021/acscatal.5b00654
ACS Catal. 2015, 5, 3973−3982

We assume that $[HCP]_c$ is a constant in the temperature range 245−260 °C. Equation 6 can be further simplified to be eq 7, in which k_2 represents the apparent reaction rate constant and can be calculated by t_c (t_c is shown in Figure S1 in the Supporting Information).

$$k_2 = \frac{k_2^i}{[HCP]_c} = \frac{1}{t_c} \tag{7}$$

ln k_2 as a function of $1/T$ is shown in Figure 4, which shows a perfectly straight line. The activation energy of the second stage of the MTH reaction is 301 kJ mol^{-1}.

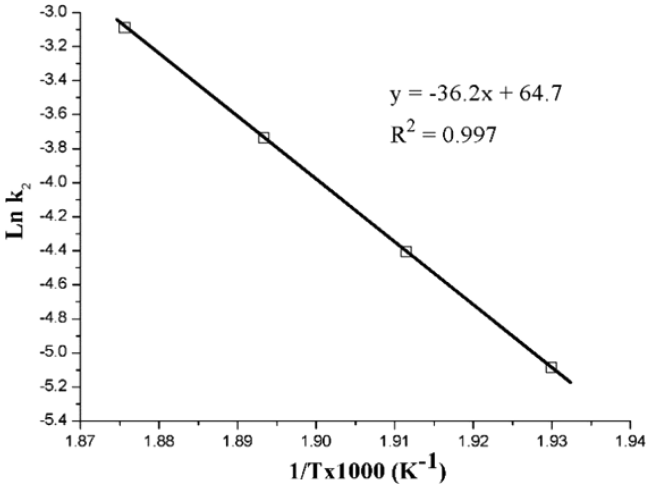

Figure 4. Arrhenius plot: the rate constant for the second stage in the MTH induction reaction in the temperature range 245−260 °C.

Kinetics and Activation Energy of the Third Stage. As can be seen from Figure 2a, the methanol conversion, if plotted in logarithmic coordinates, is a linear function of TOS. Thus, the autocatalysis reaction rate can be directly expressed as

$$\ln\ x_A = -k_3 t + B_0 \tag{8}$$

$$x_A = Be^{-k_3 t} \tag{9}$$

where k_3 is the apparent reaction rate constant, which can be obtained from Figure 5. ln k_3 as a function of $1/T$ is depicted in Figure 6. The activation energy of the autocatalysis reaction stage is 234 kJ mol^{-1}.

The linear relationships between ln k and $1/T$ for all three reaction stages in fact indicate that the hypothesis of three stages in the induction period at low reaction temperatures is reasonable. A comparison of the kinetics for three reaction stages shows that the activation barrier for the first stage is relatively low (153 kJ mol^{-1}), which means that methane and ethene are relatively easily formed over the fresh catalyst at the beginning of the reaction. The formation of the first species with a C−C bond is likely related to methane and ethene products during the first stage. After the formation of the species with a C−C bond, a series of complex reactions such as methylation, hydrogen transfer, and cyclization may occur to further produce the active HCP species. The activation energy for methanol conversion at the second reaction stage (301 kJ mol^{-1}) is higher than that at the other two stages, indicating that the formation of the HCP species is the rate-controlling step during the induction period. The formation of a certain amount of HCP species is required before the onset of the autocatalysis reaction, and thereafter the activation energy will be reduced to 234 kJ mol^{-1}.

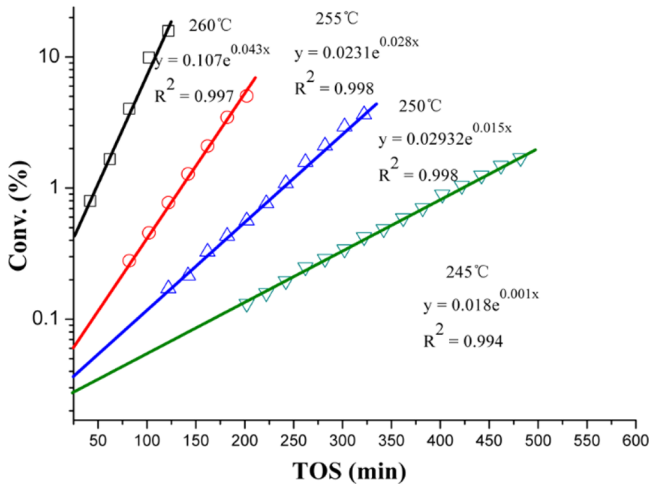

Figure 5. Conversion of methanol over HZSM-5 zeolite as a function of TOS at different reaction temperatures during the third stage of the MTH induction reaction.

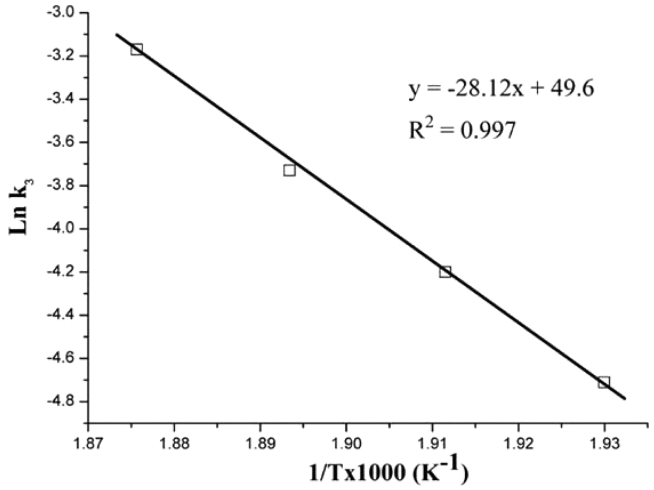

Figure 6. Arrhenius plot: the rate constant for the third stage in the MTH induction reaction in the temperature range 245−260 °C.

Note that the activation energy of the autocatalysis reaction stage is higher than that of the first stage, where the C−C bond formation most likely occurs; we can conclude that olefins might be much more easily formed at the first stage than at the third stage. As we know, the catalyst surface varies with prolonged reaction time during methanol conversion. At the beginning of the reaction, some strong acid sites on the fresh catalyst surface may favor the initial C−C bond formation at the first stage. Once these active sites are occupied or covered, they can hardly be recovered. As a result, even at the first stage the initial C−C bond formation can occur; a continuous catalysis over these strong active sites cannot last, as a limited amount of active sites is available. This is confirmed by the lower methanol conversion either after the initial reaction of methanol at the first stage or after HCP species accumulation at the second stage. To realize continuous catalysis of methanol conversion, a complete catalytic cycle is required with the involvement of HCP species. In this way, the HCP species as the cocatalyst or reaction center can be recovered during the reaction and the methanol reaction can proceed continuously.

DOI: 10.1021/acscatal.5b00654
ACS Catal. 2015, 5, 3973−3982

However, further research is still required to clarify how the energy barrier affects the three stages, due to the complexity and uncertainty of the compositions in the reaction. Nevertheless, the observations in this work provide some important information on the MTH reaction mechanism, especially the development of the induction period and the origin of the generally known autocatalysis reaction.

Effects of Cofeeding Aromatics on MTH Induction Period. *Effect on the Methanol Conversion.* It is known that the HCP species are mainly aromatic substances and are generated in the induction period. In principle, addition of aromatic species to the reaction system should shorten the induction period. Methylbenzenes and methylnaphthalenes are active HCP species.[70,71] Lower methylbenzenes with smaller size such as benzene, toluene, and *p*-xylene, which can diffuse without limitation in HZSM-5 zeolite and increase the activity, were selected in the cofeeding reaction. The introduced amount was 4 ppm (molar) for all cases.

Figure 7 shows the methanol conversion as a function of TOS when cofeeding different aromatics. As can be seen, the

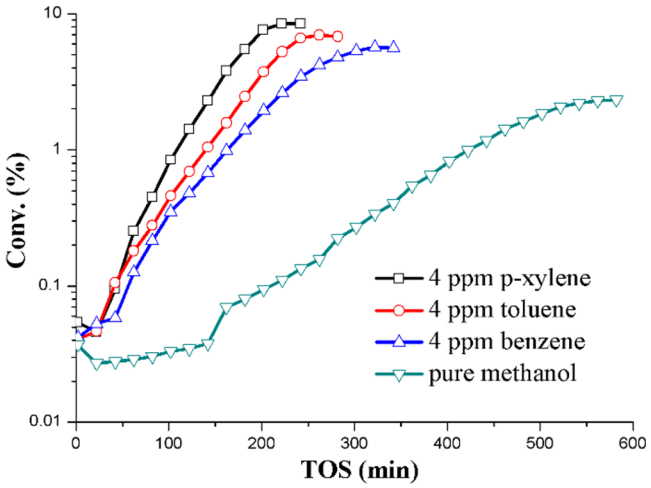

Figure 7. Conversion of methanol over HZSM-5 zeolite as a function of TOS at 245 °C with the addition of 4 ppm (molar) of benzene, toluene, and *p*-xylene into the methanol feed.

MTH induction period could be remarkably shortened and the maximum methanol conversion increased by adding only 4 ppm of aromatics. Cofeeding of benzene shows the weakest effect, while cofeeding of *p*-xylene exhibits the strongest effect among the three additives. McCann et al. reported that the 1,1,2,4,6-pentamethylbenzenium cation is an active HCP species in HZSM-5,[72] which might be generated through methylation of benzene, toluene, and *p*-xylene. It is obvious that the formation of 1,1,2,4,6-pentamethylbenzenium cation from *p*-xylene methylation requires the least methylation steps. Since all of the introduced aromatics can diffuse into the channels of ZSM-5 zeolite, the added small amount of methylbenzenes may influence the induction period in two possible ways: prompt the formation of highly active HCP species and/or act directly as HCP species. It has been proven that the organic impurities, especially aromatic impurities in methanol, can affect the induction period greatly.[3]

Effect on the Product Distribution. The effect of cofeeding a ppm amount of aromatics on the product distribution in the MTH reaction has also been investigated. Figure 8 depicts the product distribution as a function of TOS at 245 °C. Similar to the reaction with only methanol feeding (Figure 2b), the main effluent products are still methane and ethene in the first and second stages and no obvious change can be observed. However, the concentrations of C_3H_6, C_4, C_5, and C_6^+ species detected in the cofeeding process are higher than those in the process with only methanol feeding. At the autocatalysis reaction stage, the selectivity to ethene and propene is almost unchanged except for the different feeding conditions.

Ilias and Bhan recently reported the reaction of dimethyl ether cofed with toluene in very low concentration at 275 °C. It is shown that the selectivity to ethene and aromatics increases while selectivity to C_4−C_7 aliphatics drops with an increase in the amount of toluene added.[20] To simulate industrial process conditions, Lercher and coauthors performed experiments with cofeeding methanol and various aromatics, including benzene, toluene, and xylenes, at 450 °C and found that the selectivity to methane, ethene, and aromatics could be elevated at the expense of the selectivity of propene and C_4^+ higher olefins. This demonstrates that cofeeding *p*-xylene propagates the aromatics-based cycle via aromatics methylation and elimination of methane and light olefins, which suppresses the olefin-based cycle.[73]

During the induction period of the MTH reaction, it has been considered that both the aromatic-based and the olefin-based reactions for olefin formation occur with difficulty. Even when a small amount of aromatics has been added to the reaction, the influence on the product selectivity is very slight in the tests. The added aromatics more likely act as active HCP species directly, which can shorten the induction period and promote the methanol conversion.

Effect on the Kinetics of the Three Stages. Figure 9 shows the methanol conversion of a series of cofeeding reactions at different temperatures (245, 250, 255, and 260 °C) as a function of TOS. For the 4 ppm (molar) benzene cofeeding reactions (Figure 9a), the start of the autocatalysis stage is advanced from 55 to 40 min and then to 22 min when the reaction temperature is elevated from 245 to 250 °C and then to 255 °C. The initial two stages are hardly detected when the temperature is above 260 °C. After introduction of the same (molar) amount of toluene (Figure 9b), a similar trend is observed. However, for the 4 ppm (molar) *p*-xylene cofeeding reactions (Figure 9c), the episode of the initial two stages is not obvious even above 250 °C.

The methanol conversion is depicted in Figure S2 in the Supporting Information as a function of TOS for the autocatalysis stage to get the kinetic parameter of the third stage. The kinetic parameters of all three stages for different cofeeding conditions are given in Table S1 in the Supporting Information. The Arrhenius plot of ln k as a function of $1/T$ is shown in Figure S3 in the Supporting Information.

The activation energies of the three stages are calculated and given in Table 2. It can be seen that the activation energy of the first stage stays almost constant, while the energy barrier of the second and third stages drops obviously after introducing 4 ppm (molar) of aromatics. However, the promoting effects at the third stage are only slightly different for the three different aromatic additives. The results reported in this work give a new perspective on the influence of aromatics on the MTH induction period. First, it has been found that the formation of methane and ethene in the initial reaction period is not promoted by the introduction of aromatics. Second, the direct introduction of aromatics accelerates the formation of HCP species, and thus the aromatic impurities in methanol may

DOI: 10.1021/acscatal.5b00654
ACS Catal. 2015, 5, 3973−3982

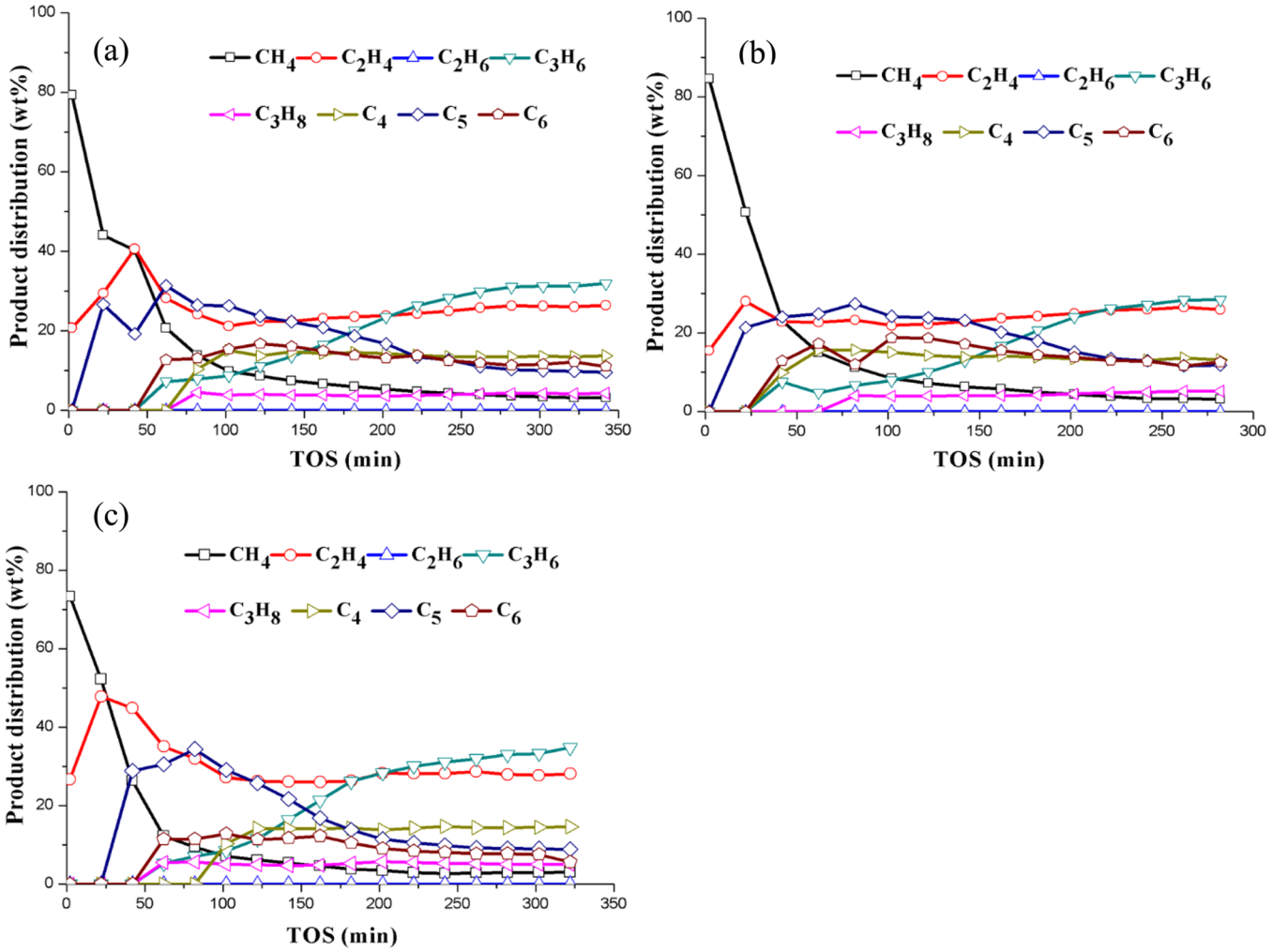

Figure 8. Product distribution versus TOS for the reactions of cofeeding methanol and 4 ppm (molar) of benzene (a), toluene (b), and *p*-xylene (c) at 245 °C.

affect the reaction essentially. At the third stage, the concentration of catalytic HCP species increases with TOS, which shows a typical feature of autocatalysis. The HCP species formation has been remarkably prompted at the third stage in the aromatics cofeeding system, which is also confirmed by the decline in activation energy. Under the aromatics cofeeding conditions, the concentration of HCP species might increase via two approaches: direct generation from methanol molecules and/or continuous introduction from the feedstock.

Measurement of the Critical Value of [HCP]$_c$. As discussed above, when the concentration of HCP species reaches a critical value, $[HCP]_c$, the autocatalysis reaction will be initiated. By cofeeding 4 ppm of benzene, toluene, or *p*-xylene, the initial two stages can be shortened significantly. The $[HCP]_c$ value should be constant at the same reaction temperature whether aromatics are cofed or not. Taking toluene as an example, we studied the effect of the amount of introduced toluene on the duration of the MTH induction period. Methanol conversions are presumably identical at the start of autocatalysis reaction for the four feeding conditions shown in Figure 10. It is clearly seen that, when the concentration of toluene is increased from 2 to 4 ppm and then to 8 ppm, the duration of the first two stages is correspondingly shortened from 95 to 50 min and then to 30 min. The methanol conversion during the autocatalysis stage is promoted, which demonstrates that the MTH induction period can be shortened considerably when the concentration of cofed toluene is increased.

The molar feeding rates of toluene in the cofeeding experiments are 4.17×10^{-9}, 8.34×10^{-9} , and 1.67×10^{-8} mol min^{-1}, which correspond to 2, 4, and 8 ppm of toluene in the feedstock, respectively. The amount of introduced aromatics during the first two stages is denoted as the amount of introduced HCP species, $[HCP]_I$, which can be directly calculated on the basis of the toluene feeding rate and initial reaction time (t_c). The amount of introduced toluene is given in Table S2 in the Supporting Information.

The linear relation between t_c and $[HCP]_I$ is depicted in Figure 11. The $[HCP]_c$ value can be obtained by extrapolating the linear relation to the duration of an induction period of 0. The critical amount of toluene is thus estimated to be 6.3×10^{-7} mol g_{cat}^{-1}. For HZSM-5 (Si/Al = 19) catalyst, the number of unit cells is 1.74×10^{-4} mol g_{cat}^{-1}, corresponding to 1 toluene molecule per 276 unit cells. This result indicates that the MTH reaction is very sensitive to aromatics in the feed or inside zeolite catalyst, which is also a possible reason some scientists believe that HCP species come from impurities.[3]

It should be noted that this method is based on the assumption that all toluene introduced will be adsorbed in the zeolite channels and act as HCP species. However, toluene will surely be transformed into other aromatic species, and the roles

DOI: 10.1021/acscatal.5b00654
ACS Catal. 2015, 5, 3973−3982

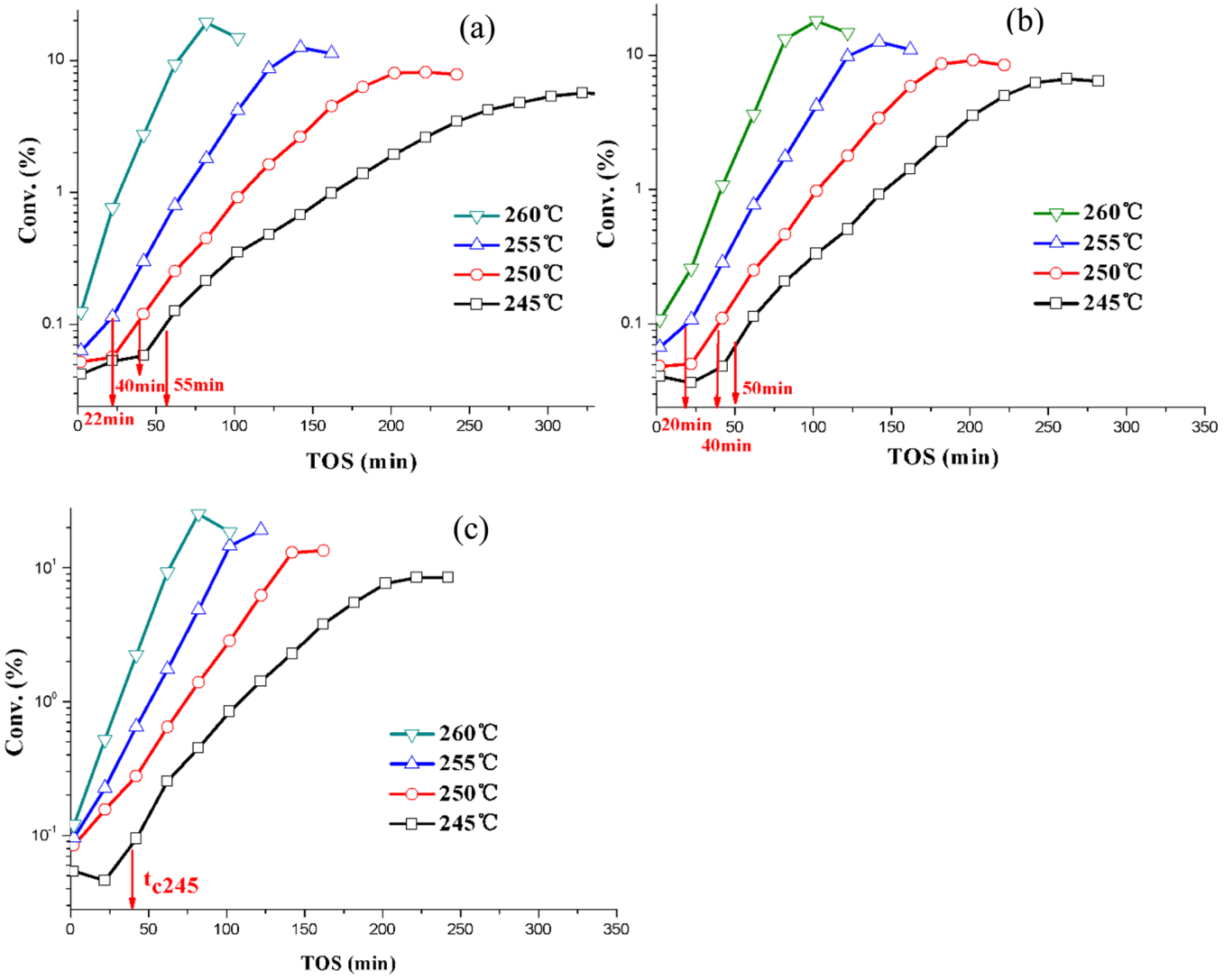

Figure 9. Methanol conversion as a function of TOS for the reactions of cofeeding 4 ppm (molar) of benzene (a), toluene (b), and *p*-xylene (c).

Table 2. Activation Energies for Different Feedstock

feedstock	E (kJ mol^{-1})		
	first stage	second stage	third stage
methanol	153	301	234
methanol with 4 ppm benzene	159	208	159
methanol with 4 ppm toluene	155	208	155
methanol with 4 ppm *p*-xylene			143

of different aromatic species in prompting the HCP species formation are different. In addition, adsorption of toluene molecules will become more difficult in zeolite at very low toluene cofeeding concentrations, especially for the case of a toluene cofeeding concentration of 2 ppm. These two reasons will bring about unavoidable deviations in this study, which can be evidenced by the fact that the curve in Figure 11 is not a perfectly straight line.

CONCLUSION

The present work provides a new insight into the MTH reaction and its induction period. At low reaction temperatures (<255 °C), the MTH induction period can be extended to as long as several hours, which enabled the direct observation and

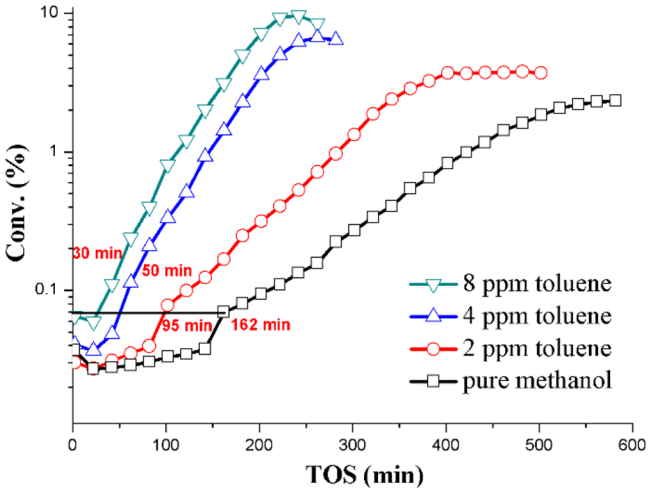

Figure 10. Influence of the concentration of cofeeding of toluene on methanol conversion at 245 °C.

detailed investigation of the MTH induction period. It is found for the first time that the induction period could be divided into three stages: the initial C−C bond formation stage, the HCP

DOI: 10.1021/acscatal.5b00654
ACS Catal. 2015, 5, 3973−3982

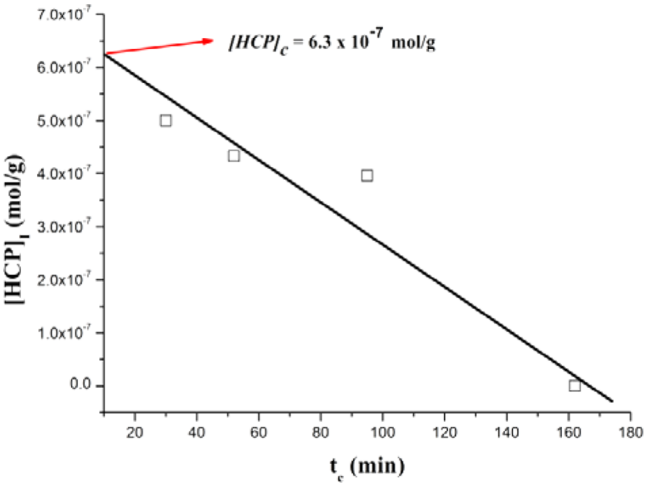

Figure 11. Influence of the amount of introduced toluene at the first two stages of the MTH induction period at 245 °C.

species formation stage, and the autocatalysis reaction stage. The kinetics for each stage has been established with newly developed methods, and the corresponding activation energies have also been calculated. This shows that the HCP species formation stage is the rate-controlling step in the MTH reaction with the highest energy barrier. A critical value of the concentration of HCP species, at which the autocatalysis reaction (at the third stage) starts, is proposed and confirmed. This critical value can be reached via the formation and/or cofeeding of HCP species on the catalyst. Cofeeding a ppm amount of benzene, toluene, or *p*-xylene causes lower activation energies for the second and third stages and in turn shortens the induction period. By altering the amount of cofed toluene, the toluene-based $[HCP]_c$ value was calculated to be as low as 1 toluene molecule per 276 unit cells for HZSM-5 (Si/Al = 19) zeolite. These findings are expected to shed some light on a detailed understanding of the induction period in the MTH reaction.

■ ASSOCIATED CONTENT

Supporting Information

The Supporting Information is available free of charge on the ACS Publications website at DOI: 10.1021/acscatal.5b00654.

More experimental results on cofeeding of aromatics, as well as the kinetic parameters for three reaction stages under different conditions (PDF)

■ AUTHOR INFORMATION

Corresponding Authors

*L.X.: e-mail, leixu@dicp.ac.cn; fax, +86 41184379318; tel, +86 41184379318.

*Z.L.: e-mail, liuzm@dicp.ac.cn; fax, +86 41184379998; tel, +86 41184379998.

Notes

The authors declare no competing financial interest.

■ ACKNOWLEDGMENTS

The authors acknowledge financial support from the National Natural Science Foundation of China (Grant No. 21273230). We also gratefully acknowledge Prof. Mao Ye, Dalian Institute of Chemical Physics, for language improvements.

■ REFERENCES

(1) Tian, P.; Wei, Y.; Ye, M.; Liu, Z. M. *ACS Catal.* **2015**, *5*, 1922−1938.
(2) Stocker, M. *Microporous Mesoporous Mater.* **1999**, *29*, 3−48.
(3) Haw, J. F.; Song, W. G.; Marcus, D. M.; Nicholas, J. B. *Acc. Chem. Res.* **2003**, *36*, 317−326.
(4) Dahl, I. M.; Kolboe, S. *J. Catal.* **1996**, *161*, 304−309.
(5) Dahl, I. M.; Kolboe, S. *J. Catal.* **1994**, *149*, 458−464.
(6) Arstad, B.; Kolboe, S. *J. Am. Chem. Soc.* **2001**, *123*, 8137−8138.
(7) Arstad, B.; Kolboe, S. *Catal. Lett.* **2001**, *71*, 209−212.
(8) Goguen, P. W.; Xu, T.; Barich, D. H.; Skloss, T. W.; Song, W. G.; Wang, Z. K.; Nicholas, J. B.; Haw, J. F. *J. Am. Chem. Soc.* **1998**, *120*, 2650−2651.
(9) Song, W. G.; Marcus, D. M.; Fu, H.; Ehresmann, J. O.; Haw, J. F. *J. Am. Chem. Soc.* **2002**, *124*, 3844−3845.
(10) Sassi, A.; Wildman, M. A.; Haw, J. F. *J. Phys. Chem. B* **2002**, *106*, 8768−8773.
(11) Sassi, A.; Wildman, M. A.; Ahn, H. J.; Prasad, P.; Nicholas, J. B.; Haw, J. F. *J. Phys. Chem. B* **2002**, *106*, 2294−2303.
(12) Seiler, M.; Schenk, U.; Hunger, M. *Catal. Lett.* **1999**, *62*, 139−145.
(13) Hunger, M.; Seiler, M.; Buchholz, A. *Catal. Lett.* **2001**, *74*, 61−68.
(14) Seiler, M.; Wang, W.; Buchholz, A.; Hunger, M. *Catal. Lett.* **2003**, *88*, 187−191.
(15) Mole, T.; Bett, G.; Seddon, D. *J. Catal.* **1983**, *84*, 435−445.
(16) Sullivan, R. F.; Sieg, R. P.; Langlois, G. E.; Egan, C. J. *J. Am. Chem. Soc.* **1961**, *83*, 1156−1160.
(17) Arstad, B.; Kolboe, S.; Swang, O. *J. Phys. Chem. A* **2005**, *109*, 8914−8922.
(18) Hemelsoet, K.; Van der Mynsbrugge, J.; De Wispelaere, K.; Waroquier, M.; Van Speybroeck, V. *ChemPhysChem* **2013**, *14*, 1526−1545.
(19) Olsbye, U.; Svelle, S.; Bjorgen, M.; Beato, P.; Janssens, T. V. W.; Joensen, F.; Bordiga, S.; Lillerud, K. P. *Angew. Chem., Int. Ed.* **2012**, *51*, 5810−5831.
(20) Ilias, S.; Bhan, A. *J. Catal.* **2012**, *290*, 186−192.
(21) Westgard Erichsen, M.; Svelle, S.; Olsbye, U. *J. Catal.* **2013**, *298*, 94−101.
(22) Ilias, S.; Bhan, A. *J. Catal.* **2014**, *311*, 6−16.
(23) De Wispelaere, K.; Hemelsoet, K.; Waroquier, M.; Van Speybroeck, V. *J. Catal.* **2013**, *305*, 76−80.
(24) Li, J. Z.; Wei, Y. X.; Chen, J. R.; Tian, P.; Su, X.; Xu, S. T.; Qi, Y.; Wang, Q. Y.; Zhou, Y.; He, Y. L.; Liu, Z. M. *J. Am. Chem. Soc.* **2012**, *134*, 836−839.
(25) Xu, S. T.; Zheng, A. M.; Wei, Y. X.; Chen, J. R.; Li, J. Z.; Chu, Y. Y.; Zhang, M. Z.; Wang, Q. Y.; Zhou, Y.; Wang, J. B.; Deng, F.; Liu, Z. M. *Angew. Chem., Int. Ed.* **2013**, *52*, 11564−11568.
(26) Bjorgen, M.; Svelle, S.; Joensen, F.; Nerlov, J.; Kolboe, S.; Bonino, F.; Palumbo, L.; Bordiga, S.; Olsbye, U. *J. Catal.* **2007**, *249*, 195−207.
(27) Svelle, S.; Joensen, F.; Nerlov, J.; Olsbye, U.; Lillerud, K. P.; Kolboe, S.; Bjorgen, M. *J. Am. Chem. Soc.* **2006**, *128*, 14770−14771.
(28) Tajima, N.; Tsuneda, T.; Toyama, F.; Hirao, K. *J. Am. Chem. Soc.* **1998**, *120*, 8222−8229.
(29) Blaszkowski, S. R.; vanSanten, R. A. *J. Am. Chem. Soc.* **1997**, *119*, 5020−5027.
(30) Lesthaeghe, D.; Van Speybroeck, V.; Marin, G. B.; Waroquier, M. *Chem. Phys. Lett.* **2006**, *417*, 309−315.
(31) Lesthaeghe, D.; Van Speybroeck, V.; Marin, G. B.; Waroquier, M. *Angew. Chem., Int. Ed.* **2006**, *45*, 1714−1719.
(32) Forester, T. R.; Wong, S. T.; Howe, R. F. *J. Chem. Soc., Chem. Commun.* **1986**, 1611−1613.
(33) Forester, T. R.; Howe, R. F. *J. Am. Chem. Soc.* **1987**, *109*, 5076−5082.
(34) Salvador, P.; Fripiat, J. J. *J. Phys. Chem.* **1975**, *79*, 1842−1849.
(35) Salvador, P.; Kladnig, W. *J. Chem. Soc., Faraday Trans. 1* **1977**, *73*, 1153−1168.

DOI: 10.1021/acscatal.5b00654
ACS Catal. 2015, 5, 3973−3982

(36) Derouane, E. G.; Dejaifve, P.; Nagy, J. B. *J. Mol. Catal.* **1978**, *3*, 453−457.
(37) Derouane, E. G.; Gilson, J. P.; Nagy, J. B. *Zeolites* **1982**, *2*, 42−46.
(38) Novakova, J.; Kubelkova, L.; Habersberger, K.; Dolejsek, Z. *J. Chem. Soc., Faraday Trans. 1* **1984**, *80*, 1457−1465.
(39) Novakova, J.; Kubelkova, L.; Dolejsek, Z. *J. Catal.* **1987**, *108*, 208−213.
(40) Kubelkova, L.; Novakova, J.; Nedomova, K. *J. Catal.* **1990**, *124*, 441−450.
(41) Salehirad, F.; Anderson, M. W. *J. Chem. Soc., Faraday Trans.* **1998**, *94*, 2857−2866.
(42) Salehirad, F.; Anderson, M. W. *J. Catal.* **1998**, *177*, 189−207.
(43) Ono, Y.; Mori, T. *J. Chem. Soc., Faraday Trans. 1* **1981**, *77*, 2209−2221.
(44) Campbell, S. M.; Jiang, X. Z.; Howe, R. F. *Microporous Mesoporous Mater.* **1999**, *29*, 91−108.
(45) Hunter, R.; Hutchings, G. J. *J. Chem. Soc., Chem. Commun.* **1985**, 886−887.
(46) Hunter, R.; Hutchings, G. J. *J. Chem. Soc., Chem. Commun.* **1985**, 1643−1645.
(47) Hutchings, G. J.; Watson, G. W.; Willock, D. J. *Microporous Mesoporous Mater.* **1999**, *29*, 67−77.
(48) Yamazaki, H.; Shima, H.; Imai, H.; Yokoi, T.; Tatsumi, T.; Kondo, J. N. *J. Phys. Chem. C* **2012**, *116*, 24091−24097.
(49) Wang, W.; Buchholz, A.; Seiler, M.; Hunger, M. *J. Am. Chem. Soc.* **2003**, *125*, 15260−15267.
(50) Zicovichwilson, C. M.; Viruela, P.; Corma, A. *J. Phys. Chem.* **1995**, *99*, 13224−13231.
(51) Sinclair, P. E.; Catlow, C. R. A. *J. Chem. Soc., Faraday Trans.* **1997**, *93*, 333−345.
(52) Shah, R.; Gale, J. D.; Payne, M. C. *J. Phys. Chem. B* **1997**, *101*, 4787−4797.
(53) Shah, R.; Payne, M. C.; Lee, M. H.; Gale, J. D. *Science* **1996**, *271*, 1395−1397.
(54) Stich, I.; Gale, J. D.; Terakura, K.; Payne, M. C. *J. Am. Chem. Soc.* **1999**, *121*, 3292−3302.
(55) Blaszkowski, S. R.; Vansanten, R. A. *J. Phys. Chem.* **1995**, *99*, 11728−11738.
(56) Blaszkowski, S. R.; vanSanten, R. A. *J. Am. Chem. Soc.* **1996**, *118*, 5152−5153.
(57) Blaszkowski, S. R.; vanSanten, R. A. *J. Phys. Chem. B* **1997**, *101*, 2292−2305.
(58) Haase, F.; Sauer, J. *J. Am. Chem. Soc.* **1995**, *117*, 3780−3789.
(59) Haase, F.; Sauer, J.; Hutter, J. *Chem. Phys. Lett.* **1997**, *266*, 397−402.
(60) Nusterer, E.; Blochl, P. E.; Schwarz, K. *Angew. Chem., Int. Ed. Engl.* **1996**, *35*, 175−177.
(61) Li, J. F.; Wei, Z. H.; Chen, Y. Y.; Jing, B. Q.; He, Y.; Dong, M.; Jiao, H. J.; Li, X. K.; Qin, Z. F.; Wang, J. G.; Fan, W. B. *J. Catal.* **2014**, *317*, 277−283.
(62) Wei, Y. X.; Zhang, D. Z.; Chang, F. X.; Liu, Z. M. *Catal. Commun.* **2007**, *8*, 2248−2252.
(63) Dai, W. L.; Dyballa, M.; Wu, G. J.; Li, L. D.; Guan, N. J.; Hunger, M. *ACS Catal.* **2015**, *119*, 2637−2645.
(64) Dai, W. L.; Wang, C. M.; Dyballa, M.; Wu, G. J.; Guan, N. J.; Li, L. D.; Xie, Z. K.; Hunger, M. *ACS Catal.* **2015**, *5*, 317−326.
(65) Langner, B. E. *Appl. Catal.* **1982**, *2*, 289−302.
(66) Lee, K. Y.; Chae, H. J.; Jeong, S. Y.; Seo, G. *Appl. Catal., A* **2009**, *369*, 60−66.
(67) Bjorgen, M.; Joensen, F.; Lillerud, K. P.; Olsbye, U.; Svelle, S. *Catal. Today* **2009**, *142*, 90−97.
(68) Sun, X. Y.; Mueller, S.; Liu, Y.; Shi, H.; Haller, G. L.; Sanchez-Sanchez, M.; van Veen, A. C.; Lercher, J. A. *J. Catal.* **2014**, *317*, 185−197.
(69) Haag, W. O.; Lago, R. M.; Rodewald, P. G. *J. Mol. Catal.* **1982**, *17*, 161−169.
(70) White, J. L. *Catal. Sci. Technol.* **2011**, *1*, 1630−1635.
(71) Yuan, C. Y.; Wei, Y. X.; Li, J. Z.; Xu, S. T.; Chen, J. R.; Zhou, Y.; Wang, Q. T.; Xu, L.; Liu, Z. M. *Chin. J. Catal.* **2012**, *33*, 367−374.
(72) McCann, D. M.; Lesthaeghe, D.; Kletnieks, P. W.; Guenther, D. R.; Hayman, M. J.; Van Speybroeck, V.; Waroquier, M.; Haw, J. F. *Angew. Chem., Int. Ed.* **2008**, *47*, 5179−5182.
(73) Sun, X. Y.; Mueller, S.; Shi, H.; Haller, G. L.; Sanchez-Sanchez, M.; van Veen, A. C.; Lercher, J. A. *J. Catal.* **2014**, *314*, 21−31.

DOI: 10.1021/acscatal.5b00654
ACS Catal. 2015, 5, 3973−3982